Original Article

Sahel Journal of Veterinary Sciences

Sahel J. Vet. Sci. Vol. 19, No. 2, Pp 13-20 (2022)

Article History
Received: 09-09-2021
Revised: 18-06-2022
Accepted: 23-06-2022
Published: 30-06-2022

Gross and Histological Studies of the Nasal Turbinates in Yankasa Sheep *(Ovis aries)* in Maiduguri, Nigeria

***Girgiri, I. A., Malah, M. K., Jiji, M. H. and Gazali, Y. A.**

Department of Veterinary Anatomy, Faculty of Veterinary Medicine, University of Maiduguri, Nigeria

* *Author for Correspondence: ibrahimgirgiri@gmail.com*

ABSTRACT

The present study was aimed at describing the anatomy of the nasal turbinates in adult Yankasa sheep using sectional anatomical planes and light microscopy. A total of 5 heads of Yankasa sheep obtained from the abattoir were used. The gross observations of the nasal turbinates were presented in midsagittal and serialized transverse sections. The nasal cavity comprised of dorsal, middle and ventral nasal turbinates. These turbinates were delineated by dorsal, middle, common and ventral nasal meatuses and presented distinct morphological details at different levels of the sectional planes. Microscopically, the mucosal lining of the nasal turbinates was divided into stratified squamous keratinized epithelium in the vestibular portion, pseudostratified columnar epithelium in the respiratory portion and olfactory pseudostratified columnar epithelium in the olfactory portion of the nasal cavity. The propria submucosa consisted of loose irregular connective tissue, having connective tissue cells, fibers, cavernous veins and cartilages. whereas the deeper part presented mixed glandular tissue of simple acinar and coiled tubular glands. The study provided basic information on gross and microscopic anatomy of the nasal turbinates in Yankasa sheep, which could serve as reference for clinical interpretation of diagnostic images of the head region of the Yankasa sheep, and for comparative anatomical studies.

Keywords: Gross anatomy; Histology; Nasal turbinates; Nasal meatus; Yankasa sheep

INTRODUCTION

The respiratory tract represents a primary pathway for infection induced by inhaled substances (Chacker, 2016). The nasal cavity as gateway to this tract, has been described as the first line of defense against invading pathogens (Yang *et al.,* 2017). It also plays a vital role in conditioning temperature, humidity and olfaction of the inspired air (Kumar *et al*., 2000).

The anatomy of the nasal cavity comprised of rostral nasal vestibule and middle nasal turbinates (Pasquini *et al*., 1999). These turbinates are complex bony plates within the nasal chamber that are covered with moist epithelium (Van Valkenburgh *et al*., 2004). The turbinates included a caudal system of ethmoidal conchae constituting the lateral labyrinth of the ethmoid bone and a rostral system of dorsal, ventral and small middle conchae (Dyce *et al*., 2010).

Understanding the morphology of the nasal cavity and associated turbinate is important in interpretation of the diseases of the upper respiratory passages and disorders of adjacent structures (Reetz *et al*., 2006), which typically presented clinical signs localized in the cavity and connected structures. Sectional anatomy has been effectively used to evaluate the accurate topographical and morphological anatomy (Smallwood *et al*., 2002; De Zani *et al*., 2010) as basis for interpreting diagnostic images for clinical applications.

The anatomy of the nasal turbinates has been studied in rabbit (Pereira *et al.,* 2011), Pig (Parkash *et al*., 2016a; Parkash and Kumar 2019) and camel (Gewaily *et al*., 2019). However, such studies have not been documented in the Yankasa sheep.

The aim of this work is to describe the anatomy of the nasal turbinates in Yankasa sheep as normal anatomical reference, using sectional anatomical planes and light microscopy.

MATERIALS AND METHODS

This study was conducted on five (5) heads of adult Yankasa sheep of either sex. The heads were obtained from Maiduguri central abattoir immediately after routine slaughter and were washed and fixed in 10% formalin. Dental eruption as described by Constantinescu (2001) was adopted to estimate the age of the samples. The fixed samples were processed as described below;

Gross Anatomical Studies

The mandibles were carefully disarticulated and removed from all collected heads to delineate the landmarks for sectioning. The heads (2) were sectioned at the midsagittal plane, whereas the remaining three (3) heads were serially sectioned transversely with the aid of electric band-saw, using landmarks presented in Figure: 1. All the sectional planes of the nasal turbinates obtained were gently cleansed to remove tissue debris using tap water and light brush. Morphological features of the nasal turbinates were studied and photographed.

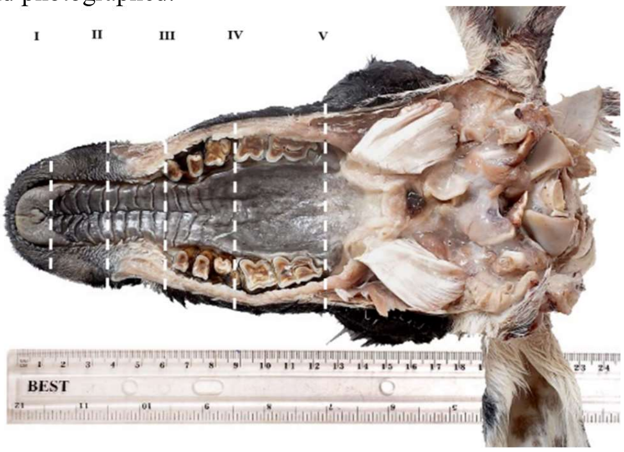

Figure 1: Landmarks of the anatomical planes of Yankasa sheep head (ventral view) showing; incisive papillae I, six palatine ridge II, first premolar III, between third premolar and first molar IV, caudal of third molar V.

Histological Studies

Tissues were collected from Alar, basal, straight folds and the nasal conchae (dorsal, middle and ventral). These were processed by routine paraffin techniques of light microscopy and sections of 5-7 micrometer (µm) were cut and stained with hematoxylin and eosin (H&E) stain (Luna, 1968). Histo-morphological feature of the sections was examined and microphotographs were taken at different magnifications.

Ethical Statement

Ethical approval was not required, as the tissue sample for the study were collected from the abattoir after routine slaughter for human consumption.

RESULTS

Gross Morphological Findings

Midsagittal Section

The nasal cavity of Yankasa sheep has quadrilateral orientation and extended from nasal vestibule to the cribriform plate of the ethmoidal bone. It was bounded dorsally by frontal and nasal bones, whereas the floor of the cavity was lined by incisive and palatine bone. The nasal cavity was divided into equal halves by nasal septum and majority of its extent was occupied by the nasal turbinates. These turbinates comprised of dorsal, middle and ventral nasal conchae. The dorsal nasal concha was situated between the dorsal and middle meatuses. It was fusiform shaped where it tapers rostral to continue as the straight fold. The middle nasal concha was situated caudal most. The rostral half enclosed a conchal sinus whereas the caudal half presented the ethmoidal labyrinth. The ventral nasal concha was situated ventral between the dorsal and ventral meatuses. The rostral continuation of this concha unites with the alar fold dorsally and basal fold ventrally. The vomeronasal organ extend from mid-level of the sixth palatine ridge to incisive papilla (Fig: 2).

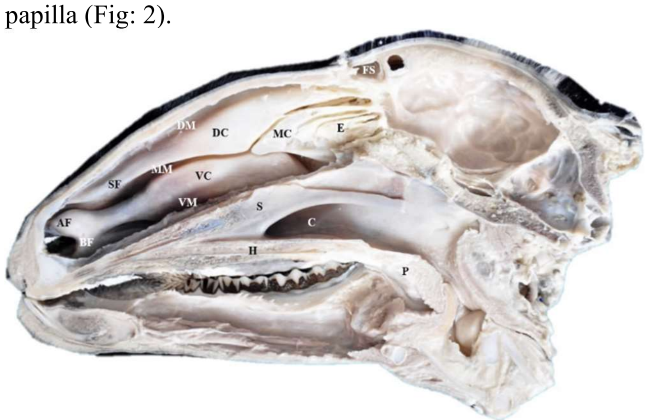

Figure 2: Mid-sagittal section of Yankasa sheep head showing; dorsal meatus DM, dorsal concha DC, frontal sinus FS, middle concha MC, ethmoidal labyrinth E, middle meatus MM, ventral concha VC, ventral meatus VM, straight fold SF, alar fold AF, basal fold BF, vomeronasal organ VO, nasal septum S, choana C, hard palate H, soft palate P.

At the level of incisive papillae

This anatomical plane showed the caudal surface of the nostril sagittally divided by the rostral portion of nasal septum. The median nasal cartilage supported the nasal septum and was surrounded by the nasal mucosa. This cartilage broadens on the dorsal and ventral margins of the nostril to form the dorsolateral and the ventral nasal cartilages which gives a characteristic shape to the dorsolateral margin of the nostril. The paired vomeronasal organ was visible as circular structures at the base of the median nasal septum (Fig: 3 A).

At the level of sixth (6^{th}) palatine ridge

This level was obtained immediately caudal to the sixth palatine ridge. The straight fold was visible extending ventromedial from the lateral wall of the nasal cavity towards the median septum. Four nasal meatuses were distinct and communicated with each other. The dorsal meatus was present as a passage between the nasal bone and the straight fold. The middle meatus was present between the straight fold and the portion of the ventral concha. The common meatus lies on either side of the median nasal septum. The ventral meatus as this level presented shallow passage below the ventral concha. The basal lamella of the ventral nasal concha extends from the lateral wall of the cavity and makes sharp bend dorsal, forming initial segment of the dorsal spiral lamella. Towards the proximal half of the median nasal septum, the nasal membrane present paired prominences forming a bulb-like structure on both side of the median septum (Fig: 3 B).

At the level of first premolar

This section was obtained rostral to the first premolar. The basal lamella of the ventral concha bifurcated giving rise to dorsal and ventral scrolls respectively. The dorsal scrolls were relatively larger and completed a single turn inward in a spiral fashion, whereas the ventral scroll completed only a half turn. The dorsolateral edges of the dorsal scrolls presented a prong-like structure. These are the rostral part of the middle conchal sinus. The middle and ventral meatuses at this level were prominent. Toward the distal half, the mucous membrane of the nasal septum expanded where its blends with cavernous sinus and the vomeronasal organ (Fig: 4 A).

At the level of third premolar

At this plane of section, the dorsal concha enlarged to enclose the dorsal conchal sinus. The dorsal scrolls of the ventral concha approximately completed a double turn. The middle portion of the median nasal septum slightly widens, whereas the proximal and distal half becomes narrowed. The palatine process of the maxilla was positioned between the ventral nasal meatus dorsal and the maxillary sinus ventral. The hard palate becomes relatively thin where it continues as the soft palate (Fig: 4 B)

At the level of third molar

This anatomical plane was obtained caudal to the third molar. The ethmoidal labyrinth presented numerous irregular scrolls that constituted caudal limit of the middle concha. Dorsal to this labyrinth was the rostral frontal sinus, which was divided arbitrarily by septa into the median, intermediate and lateral sinus. The median nasal septum was deficient distally giving rise to the wide choanae. The maxillary sinus was visible at this plane of section (Fig: 4 C).

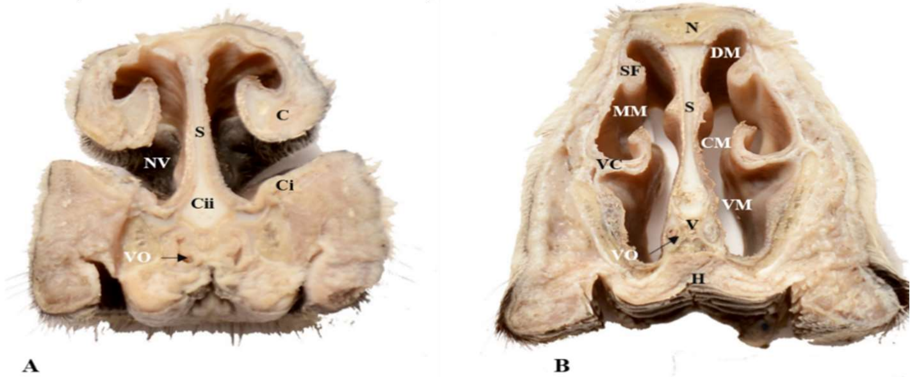

Figure 3 A-B: Transverse section (caudal view) of nasal cavity of Yankasa sheep. **A**. at the level of incisive papillae showing; nasal vestibule NV (left), dorsolateral nasal cartilage C, ventrolateral nasal cartilage Ci, median nasal cartilage Cii, nasal septum S. **B**. At the level of six palatine ridge showing; nasal bone N, dorsal meatus DM, middle meatus MM, straight fold SF, nasal septum S, ventral nasal conchae VC, common meatus CM, ventral meatus VM, vomer V, vomeronasal organ VO, hard palate H.

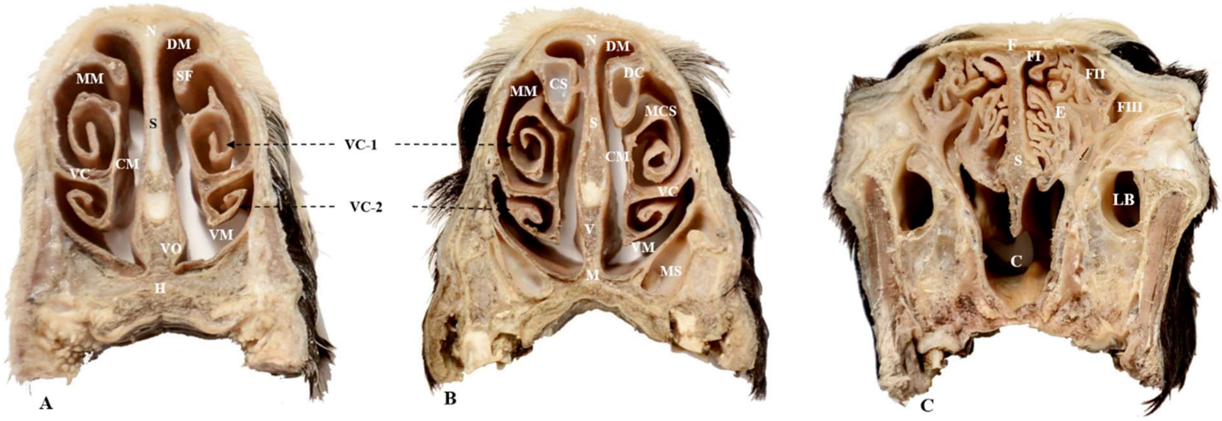

Figure 4 A-C: Transverse section of nasal cavity of Yankasa sheep. **A**. at the level of first premolar showing; nasal bone N, dorsal meatus DM (right), straight fold SF, middle meatus MM, basal lamella of ventral conchae VC, dorsal scroll of ventral concha VC-1, ventral scroll of ventral concha VC-2, nasal septum S, common meatus CM, ventral meatus, VM, vomeronasal organ VO, hard palate H. **B**. At the level of third premolar showing; nasal bone N, dorsal meatus DM, dorsal conchae DC, dorsal conchal sinus CS, nasal septum S, middle conchal sinus MCS, ventral conchae VC, vomer V, maxillary sinus MS, palatine process of maxilla M. **C**. At the level of third molar showing; frontal bone F, medial, intermediate, lateral frontal sinus (FI-III), ethmoidal labyrinth E, nasal septum S, lacrimal bulla B, choanae C.

Histological Findings

Alar Fold

Alar fold was lined by stratified squamous non-keratinized epithelium. The propria submucosa consisted of loose irregular connective tissue which comprised of connective tissue cells, fibers, cavernous veins and fine blood capillaries. Towards the deeper part, the propria presented glandular acini in form of lobules separated by interlobular connective tissue and their associated intra and interlobular ducts. Adjacent to the glandular tissue was hyaline cartilage surrounded by perichondrium. The chondrocytes at the surface were small with lightly basophilic nuclei, whereas those within the deep surface of the cartilage were larger with darkly basophilic spherical nuclei. The fibrous layer of the perichondrium which consisted of fibroblast and strands of irregular fibers were also observed (Fig: 5 A-C).

Basal fold

The mucosa of the basal fold was lined by stratified cuboidal epithelium. The basal surface of the epithelium presented linearly arranged basal cells. The free surface of this epithelium was having uniform dimension. The sup-epithelial portion of the propria submucosa comprised of loose irregular connective tissue consisting of connective tissue cells and variable number of fibers. Whereas, the deeper portion presented clusters of glandular tissue separated by interglandular connective tissue. At some places, cluster of adipose tissue were observed in between glandular tissue and hyaline cartilage. The structural detail of the hyaline cartilage was similar to findings observed in alar fold (Fig: 6 A-C).

Straight fold

The straight fold was lined by stratified squamous slightly keratinized epithelium. At interval, the epithelium invaginated giving rise to presences of papillary pegs. The propria submucosa consists of loose irregular connective tissue comprising of connective tissue cells and fibers, whereas the deeper part presented cavernous veins of variable sizes, glandular tissue and their intra and interlobular ducts (Fig: 7 A&B).

Dorsal Nasal Concha

The middle portion of the dorsal nasal conchae presented an irregular osseous plate which divided this concha into outer and inner surface, each of which was lined by pseudostratified columnar ciliated epithelium with goblet cells. The propria submucosa beneath the epithelial lining on the inner surface presented loose irregular connective tissue comprising of connective tissue cells, few fibers and more deeply cavernous veins of variable sizes. Whereas, the propria submucosa on the outer surface consisted of slightly dense irregular connective tissue. At some places, this propria was interrupted by short duct of simple acinar glands that connect with the surface epithelium. Towards the deeper portion of the propria, glandular ducts and variable sized cavernous veins were similarly observed (Fig: 8 A-C).

Middle Nasal Concha

The middle concha was lined by olfactory pseudostratified columnar epithelium. The epithelium comprised of linearly arranged basal cells and supporting cells towards the mid portion of the epithelium. The propria submucosa consisted of loose irregular connective tissue having connective tissue cells and numerous cross-sectional profiles of simple coiled tubular gland and their associated glandular ducts. In addition, different sized cavernous veins were observed towards the deeper portion of the concha. (Fig: 9 A & C)

Ventral Nasal Concha

The epithilium lining on the rostral two-third (basal fold) of the ventral nasal concha presented transition zone, where the epithelium modified from stratified squamous to cuboidal epithelium. Towards the caudal portion, the epithelium of the ventral concha becomes pseudostratified epithelium with numerous goblet cells. The sub-epithelial part of propria submucosa at the rostral two-third was having a slightly dense irregular connective tissue comprising of connective tissue fibers and few cells, whereas towards the deeper part presented few cavernous veins. The propria submucosa on the caudal-third consists of loose irregular connective tissue, whereas deeper part presented coiled tubular glands, intra and interlobular ducts as well as few cavernous vein (Fig: 10 A-C).

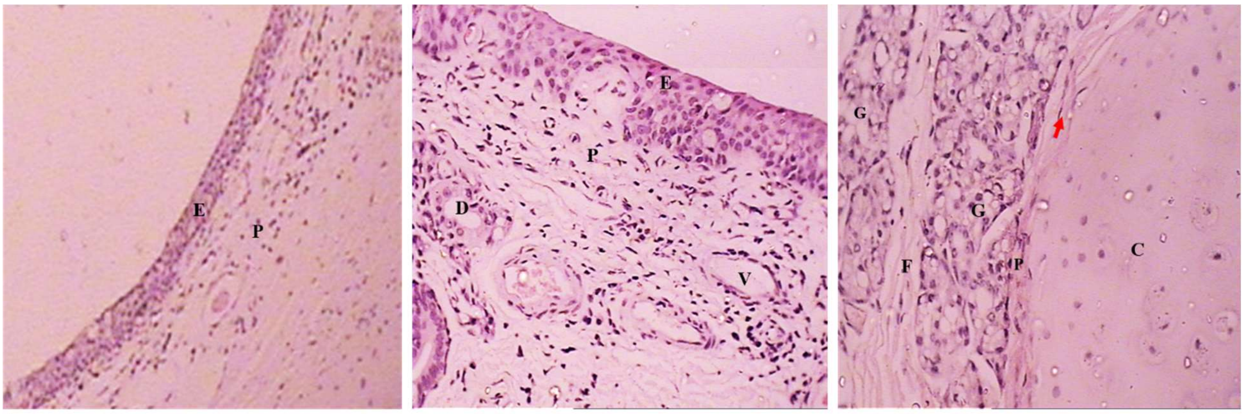

A B C

Figure 5: Photomicrograph of alar fold showing; A. stratified squamous keratinized epithelium (E) H. & E. x 100; B. propria submucosa (P) having interlobular ducts (D) cavernous vein (V) H. & E. x 400; C. deep part of propria showing glandular acini (G) interlobular connective tissue (F), perichondrium (P) showing fibrous layer (red arrow), hyaline cartilage (C) H. & E. x 400.

DISCUSSION

The nasal cavity comprised of dorsal and ventral nasal turbinates and the ethmoturbinates (Habel, 1989) described as important diagnostic features of the class Mammalia (Valkenburgh *et al*., 2004). The nasal cavity was cylindrical shaped in Yankasa sheep, divided by the sagittal median nasal septum into equal halves. In the ox and dog, the caudal half of this median nasal septum does not meet the palate, thus separated from the floor of the nasal cavity (Dyce *et al*., 2010).

The vomeronasal organ in the present study extended from third premolar, whereas in the pig from six palatine ridge (Parkash *et al*., 2016b) to the incisive papillae on either side of the ventral aspect of the median nasal septum. It has been stated that such position facilitates the olfaction of sexual odors and allows easy passage of the pheromones to the organ (Moawad *et al*., 2017). The caudal extends of the vemoronasal organ varied among species; camel (Karimi *et al*., 2014), male red fox (Karimi *et al*., 2016).

The dorsal nasal conchae (endoturbinate I) in Yankasa sheep were the longest, extended rostral by the straight fold as reported in Ossimi sheep by Alsafy *et al*. (2021), camel (Gewaily *et al*., 2019), Red fox (Mahdi and Zayed, 2020). Whereas in donkey, the rostral portion of the dorsal nasal concha presented scrolls, surrounding recesses of the nasal cavity (El-Gendy and Alsafy, 2010). In Tuj sheep, the dorsal conchae extend between interalveolaris to zygomatic arch (Demiraslan *et al*., 2020). The caudal portion of the dorsal conchae enclosed the conchal sinus as reported in previous studies; donkey (El-Gendy and Alsafy, 2010), camel (Gewaily *et al*., 2019).

The dorsal conchal sinus in Yankasa sheep, extended from the level of first premolar to caudal surface of third premolar as reported in Gaddi sheep (Pathak and Rajput, 2015) and pig (Parkash *et al*., 2016a). However, Awaad *et al*. (2019) in Egyptian native sheep reported that the sinus extends up to the caudal border of the last molar tooth. The dorsal turbinate in donkey further divided into rostral and caudal parts by dorsal conchal septum (Metwally *et al*., 2019).

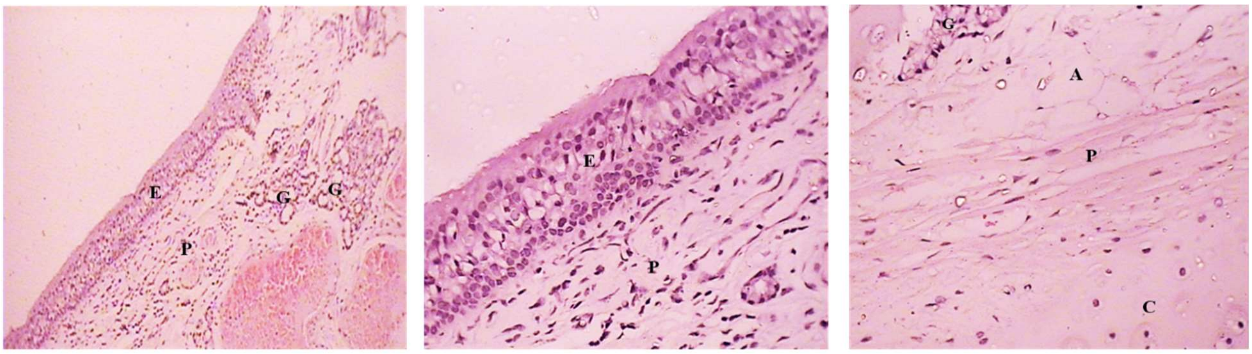

A B C

Figure 6: Photomicrograph of basal fold showing; A. stratified cuboidal epithelium (E) H. & E. x 100; B. higher magnification showing the surface epithelium (E) propria submucosa (P) with loose irregular connective tissue H. & E. x 400; C. glandular acini (G), adipose tissue (A) perichondrium (P) cartilage (C) H. & E. x 400.

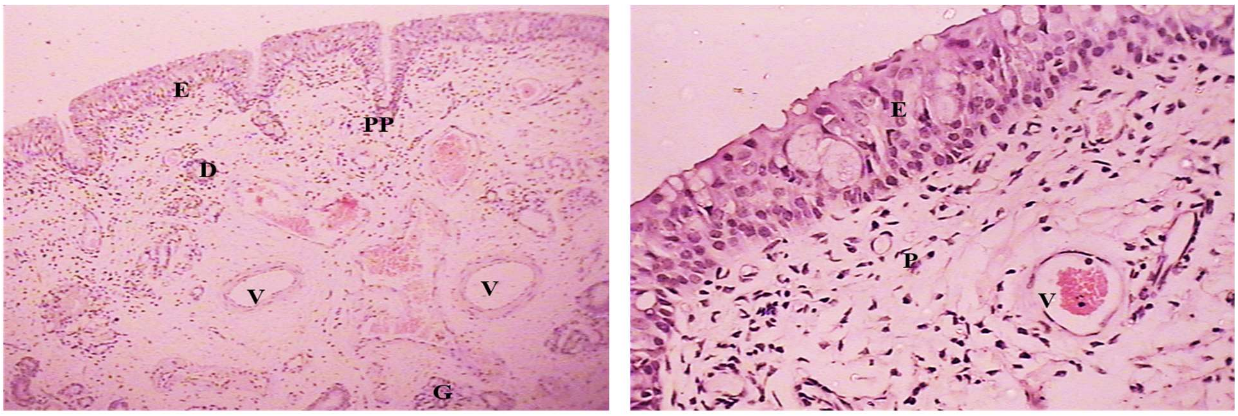

A B

Figure 7: Photomicrograph of straight fold showing; A. stratified squamous keratinized epithelium (E) having papillary pegs (PP) at intervals H. & E. x 100; B. Higher magnification showing propria submucosa (P) with loose connective tissue and cavernous vein (V) H. & E. x 400.

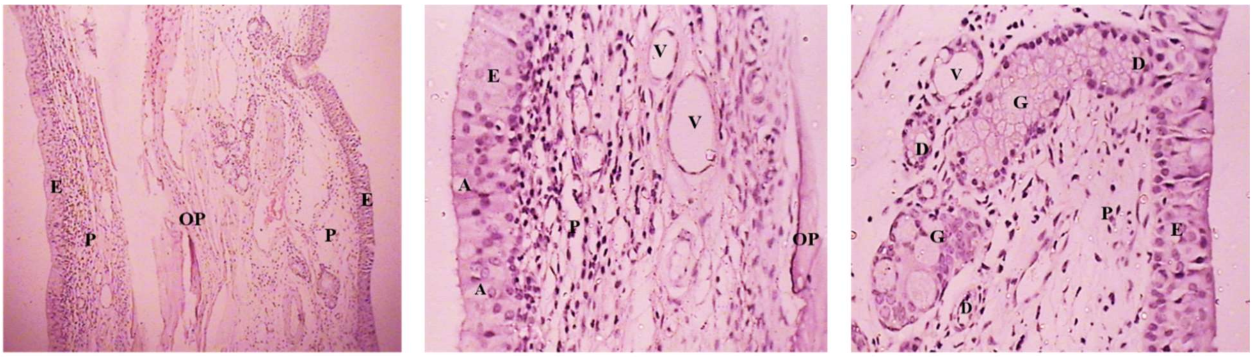

A B C

Figure 8: Photomicrograph of dorsal nasal conchae showing; A. Pseudostratified columnar ciliated epithelium with goblet cells (E) propria submucosa (P) osseous plate (OP) H. & E. x 100; B. higher magnification of the pseudostratified epithelium (E) showing goblet cells (A)

propria mucosa (P) with loose connective tissue having cavernous veins (V) H. & E. x 400; C. propria mucosa (P) with slightly dense connective tissue having simple acinar gland connected by short duct to surface epithelium (G), interlobular ducts (D) cavernous veins (V) H. & E. x 400.

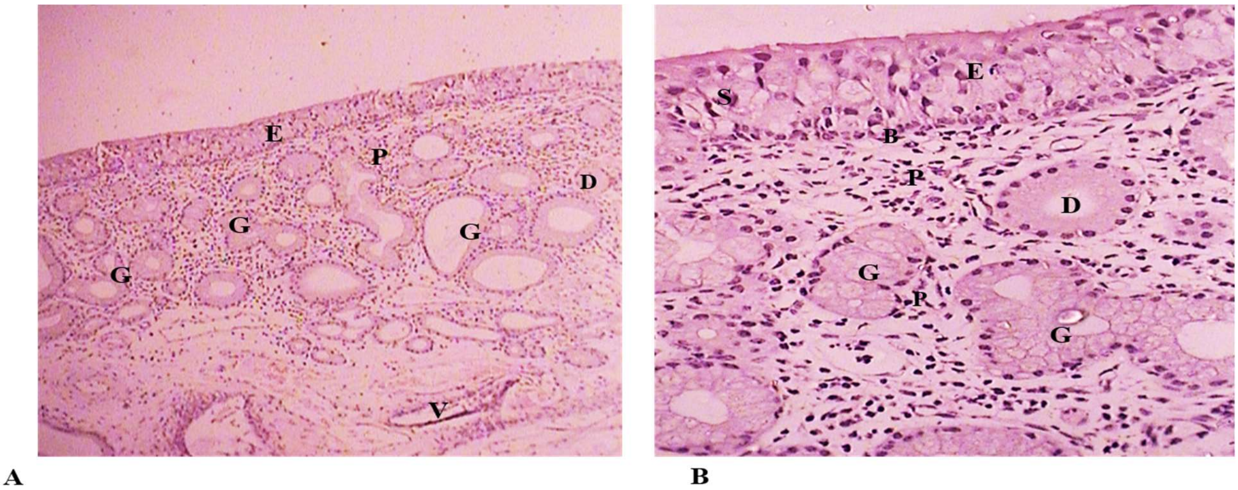

Figure 9: Photomicrograph of middle nasal conchae showing; A. olfactory pseudostratified columnar epithelium (E) propria submucosa (P) having cross sectional profiles of simple coiled tubular gland (G) cavernous vein (V) H. & E. x 100; B. higher magnification of olfactory epithelium (E) showing basal cells (B), supporting cells (S) propria submucosa (P), having coiled tubular gland (G) interglandular ducts (D) H. & E. x 400.

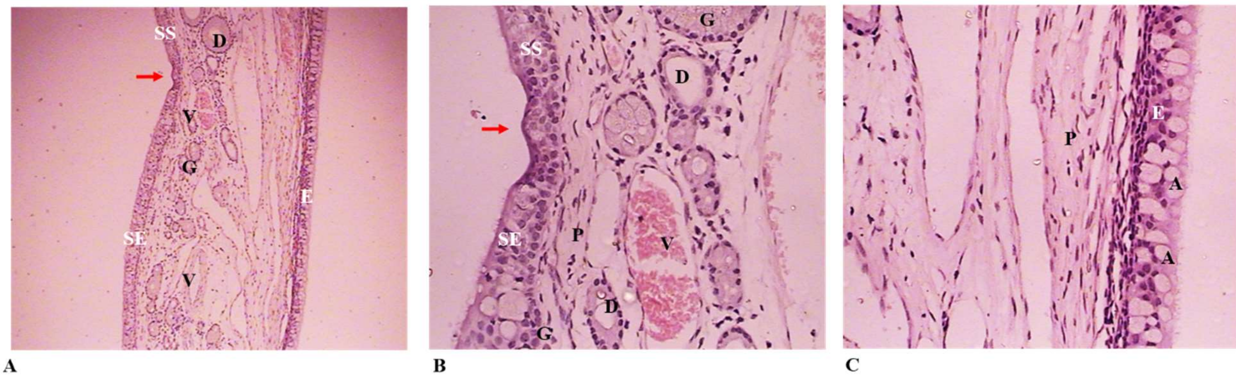

Figure 10: Photomicrograph of ventral nasal conchae; A. rostral two-third (basal fold) showing transition zone (red arrow) from stratified squamous epithelium (SS) to stratified cuboidal epithelium (SE), towards the caudal portion showing pseudostratified columnar epithelium (E) with goblet cells (A) H. & E. x 100; B. higher magnification of the transition zone (red arrow) propria submucosa (P) with slightly dense connective tissue, coiled tubular glands (G) inter/intra glandular ducts (D) cavernous vein (V) H. & E. x 400; C. caudal portion showing higher magnification of pseudostratified columnar ciliated epithelium (E) with numerous goblet cells (A) propria submucosa (P) H. & E. x 400.

The rostral portion of the ventral nasal conchae in Yankasa sheep bifurcated into dorsal alar fold and ventral basal fold as observed in Gaddi sheep (Pathak and Rajput, 2015) and camel (Gewaily *et al*., 2019). In the buffaloes and camels, this concha divided into *pars dorsalis* and *pars ventralis*, (Metwally *et al*., 2019). Whereas In the pig, it was fusiform shaped and shorter (Parkarsh *et al*., 2016a), branched in red fox (Mahdi and Zayed, 2020), and appeared nearly S-shape along its length in camel (Gewaily *et al*., 2019). The ventral conchal sinus was absent in Yankasa as reported in in buffalo (Alsafy *et al*., 2013), pig (Parkarsh *et al*., 2016a) and sheep (Awaad *et al*., 2019). In donkey, the ventral conchal sinuses are enclosed within the caudal portion, whereas the rostral portion presented scroll surrounding recesses (El-Gendy and Alsafy, 2010).

The caudal half of the middle nasal meatus, bifurcated into dorsal and ventral meatuses by the rostral portion of the middle nasal as observed in pig (Parkash *et al*., 2016a) and camel (Gewaily *et al*., 2019). The ventral nasal meatus was situated between the ventral nasal concha and the floor of the nasal cavity. It has been stated that the pharynx can be assessed by the passage of nasogastric tube and endoscope via the ventral meatus (Konig and Liebich, 2004), whereas the dorsal and middle nasal meatuses are dead ends (Constantinescus, 2001).

The lining epithelium modification of the nasal turbinates in the presented study were earlier observed in other domestic mammals; horse (Kumar *et al*., 2000), rabbit (Pereira *et al*., 2011), pig (Parkash and Kumar, 2019). In our findings, the straight and alar folds were lined with stratified squamous keratinized epithelium. Whereas in the pig, it transitioned into the pseudostratified ciliated columnar epithelium with goblet cells (Parkash and Kumar, 2019). According to Gewaily *et al*. (2019), the stratified keratinized epithelium offer protection to the underlying tissues against tear and fluid evaporation. The stratified cuboidal epithelium of the basal fold observed in Yankasa sheep, had been reported previously in bovines (Adams, 1986) and camel (Gewaily *et al*., 2019).

The loose irregular connective tissue of propria submucosa, fine blood capillaries, few venous caverns and glandular acini were also observed in pig (Parkash and Kumar, 2019). The epithelium of the ventral nasal turbinates in our findings, showed transition zone from stratified squamous to cuboidal epithelium as reported in camel (Gewaily *et al*., 2019). The caudal portion of dorsal and ventral nasal turbinate in the pig was infiltrated by lymphoid cells and modified into follicle associated epithelium (FAE) (Parkash and Kumar, 2019). The middle nasal turbinates in this study presented olfactory pseudostratified columnar epithelium as observed in rabbit (Pereira *et al*., 2011), whereas in pig, infiltration of lymphocytes was seen in between the epithelial cells (Parkash and Kumar, 2019). The structures in the propria submucosa of the nasal turbinates as well as the deeper portions were similar to findings in other domestic mammals as reported earlier.

Conclusions

The study demonstrated two well developed ethmoturbinates (dorsal and middle nasal conchae) in Yankasa sheep which arises from the dorsal and lateral wall of the cribriform plate of the ethmoid bone, and the ventral nasal concha which form part of the maxilla as maxilloturbinates. The epithelial lining of the ethmoturbinates were vestibular (stratified squamous keratinized epithelium) at the rostral half, respiratory (pseudostratified columnar ciliated epithelium) at the middle portion and olfactory (olfactory pseudostratified epithelium) at the caudal part. The maxilloturbinates showed transitional epithelium of stratified squamous to cuboidal epithelium at rostral half and respiratory epithelium towards the caudal extremities.

Conflict of Interest

The authors have no conflict of interest to declare.

Authors Contributions

IAG designed the study and interpreted findings, MHJ collected and processed the specimens, MMK and YAG were involved in drafting and revision of the manuscript.

REFERENCES

Adams, D.R. (1986). Transitional epithelial zone of the bovine nasal mucosa. *American Journal of Anatomy*,176 (2): 159-170.

Alsafy, M., Madkour, N., Abumandour, M, El-Gendy, S. and Karkoura, A. (2020). Anatomical description of the head in Ossimi Sheep: Sectional anatomy and Computed Tomographic approach. *Morphologie*, 105: 29-44. https://doi.org/10.1016/j.morpho.2020.06.008.

Alsafy, M.A.M., El-Gendy, S.A.A. and El Sharaby, A.A. (2013). Anatomic reference for computed tomography of paranasal sinuses and their communication in the Egyptian buffalo (*Bubalus bubalis*). *Anatomia Histologia Embryologia*, 42(3): 220-231. https://doi.org/10.1111/ahe.120056.

Awaad A.S., Abdel Maksoud, M.K.M. and Fathy, M.Z. (2019). Surgical anatomy of the nasal and paranasal sinuses in Egyptian native sheep (*Ovisaries*) using computed tomography and cross sectioning. *Anatomia Histologia Embryologia*, 48:279-28. https://doi.org/10.1111/ahe.12436.

Chacker, A. (2016). Anatomy and microanatomy of tonsils. *Encyclopedia of Immunobiology*, 3: 420-26. https://doi.org/10.1016/B978-0-12-374279-7.07005-3.

Constentinicus, G.M. (2001). Guide to regional ruminant anatomy based on the dissection of the goat. Iowa state university press. 206-208.

Demiraslan, Y., Dayan, M.O, Ertilav, K, Akbulut, Y, Özkadif, S. and ÖZGEL, O. (2020). Computed Tomography Imaging of Cavum nasi and Sinus paranasales in the Tuj Sheep. *Dicle Üniversitesi Veteriner Fakültesi Dergisi,* 13(1): 1-8.

De Zani, D., S. Borgonovo, M. Biggi, S. Vignati, M. Scandella, S. Lazzaretti, S. Modina, and D. Zani. (2010). Topographic comparative study of paranasal sinuses in adult horses by computed tomography, sinuscopy, and sectional anatomy. *Veterinary Research Communication*, 34(1): S13–S16.

Dyce, K.M., Sock, W.O. and Wensing, C.S.G. (2010). Textbook of Veterinary anatomy 4th ed. W.B sounders company Philadelphia.

El-Gendy, S.A. and Alsafy, M.A.M. (2010). Nasal and Paranasal Sinuses of the Donkey: Gross anatomy and Computed Tomography. *Journal of Veterinary Anatomy*, 3 (1): 25-41.

Gewaily, M.S., Hadad, S.S. and Soghay, K.M. (2019). Gross, histological and scanning electron morphological studies on the nasal turbinates of one humped camel (*Camelus dromedarius*). *Bioscience Research*, 16 (S1-2): 107-120. https://doi.org/10.13140/RG.2.2.14906.13769.

Habel, R.E. (1989). Guide to the dissection of domestic ruminants. 1529 Ellis Hollow Road Ithaca, NY 14850. 191-192.

Karimi, H., Ale-Hashim, R.M., Ardalani, G, Sadrkhanloo, R. and Hayatgheibi, H. (2014). Structure of vomeronasal organ (Jacobson's organ) in male *Camelus Domesticus Var. dromedarispersica*. *Anatomia. Histologia. Embryologia*, 43: 423-428.

Karimi, H., Hassanzadeh, B. and Razmaraii, N. (2016). Structure of vomeronasal organ (Jacobson's organ) in male red fox (*Vulpes vulpes*). *Anatomical Science*, 13(1): 47-54.

Kumar, P., Timoney, J, Southgate, H. and Sheoran, A. (2000). Light and scanning electron microscopic studies of the nasal turbinates of the horse. *Anatomia. Histologia. Embryologia*, 29 (2):103-109.

Konig, H.A. and Liebich, H. (2004). Text Book and Color Atlas of Veterinary Anatomy of Domestic Mammals.

Luna, L.G. (1968). Manual of Histologic Staining Methods of Armed Forces Institute of Pathology. 3rd edn., McGraw Hill Book Co., New York.

Mahdy, M.A.A. and Zayed, M. (2020). Computed tomography and cross-sectional anatomy of the head in the red fox (*Vulpes vulpes*). *Anatomia. Histologia. Embryologia*, 00: 1-10. https://doi.org/10.1111/ahe.12565.

Moawad, U.K., Awaad, A.S. and Abedellaah, B.A. (2017). Morphological, histochemical and computed tomography on the vomeronasal organ (Jacobson's organ) of Egyptian native breeds of goats (*Capra hircus*). *Beni-seuf University Journal of Basic and Applied Science,* 6: 173-183. https://doi.org/10.1016/j.bjbas.2017.03.003.

Metwally, M.A., Hussieni, H.B, Kassab, A.A. and Eshrah, E.A. (2019). Comparative Anatomy of the Nasal Cavity in Buffaloes, Camels and Donkeys. *Journal of Advanced Veterinary Research* 9(2): 69-75.

Nickel, R., Schummer, A. and Seiferle, E. (1979). The viscera of the domestic mammals 2nd revised ed. Verlag Paul Parey. Berlin, Hamburg. 211-281.

Parkash, T., Kumar, P. and Gurdial, S. (2016a). Gross anatomical studies on the nasal turbinate of young pigs (*Susscrofa*). *Haryana Veterinaria*, 55(2): 130-132.

Parkash, T., Kumar, P. and Gurdial, S. (2016b). Gross anatomical and light microscopical Studies on vomeronasal organ of young Pigs (*Susscrofa*). *Veterinary Research International* 4(2): 84-88.

Parkash, T. and Kumar, P. (2019). Histological and histochemical studies on the nasal cavity of the young pigs (Susscrofa). *Indian Journal of Veterinary Anatomy* 31 (1): 40-43.

Pasquini, C., Spurgeon, T. and Pasquini, S. (1999). Anatomy of domestic animals systemic and regional approach 9th ed. SUDZ publishing. 307.

Pathak, V. and Rajput, R. (2015). Gross and morphometrical study on the external and internal nares of Gaddi sheep. *Himachal Journal of Agricultural Research*, 41(2): 156-159.

Pereira, M.E., Nicholas, P., Macri, N.P. and Dianne M. Creasy, M.D. (2011). Evaluation of the Rabbit Nasal Cavity in Inhalation Studies and a Comparison with Other Common Laboratory Species and Man. T*oxicologic Pathology*, 39: 893-900. https://doi.org/10.1177/0192623311409594.

Reetz, J. A., Mai, W., Muravnick, K. B., Goldschmidt, M. H., and Schwarz, T. (2006). Computed tomographic evaluation of anatomic and pathologic variations in the feline nasal septum and paranasal sinuses. *Veterinary Radiology and Ultrasound*, 47: 321-327. https://doi.org/10.1111/j.1740-8261.

Smallwood, J. E., Brett, C, Wood, B.C, Taylor, W.E. and Lloyd, P. (2002). Anatomic reference for computed tomography of the head of the foal. *Veterinary Radiology and Ultrasonography*, 43: 99-117.

Van Valkenburgh, B., Theodor, J, Friscia, A, Pollack, A. and Rowe, T. (2004). Respiratory turbinates of canids and felids: a quantitative comparison. *Journal of Zoology*, 264 (3): 281- 293. https://doi.org/10.1017/S0952836904005771.

Yang, J., Dai, L., Yu, Q. and Yang, Q. (2017). Histological and anatomical structure of the nasal cavity of Bama minipigs, *PLoS ONE* 12: 1-14. https://doi.org/10.1371/journal.pone.0173902.